# ($^{99m}$Tc)-PSMA. Evaluation of primary and metastatic prostate tumors. Chemical, radiochemical and clinical study.

Carlos O. Cañellas[1], Sebastián Ardanaz[1], Mauro Bernini[1], Javier Prieto[1], Pablo Pérez Valenti[1], Daylen Espinosa Martínez[1], Dailenys Espinosa Martínez[1], Silvina Racciopi[2].
[1] Tecnonuclear s.a-Ecker-Ziegler, Buenos Aires, Argentina
[2] IAF (Alexander Fleming Institute), Buenos Aires, Argentina

## ABSTRACT

The work is based on the sequence of stages that the Registry of Medicinal Specialties (REM) of the National Administration of Drugs, Food and Medical Technology (ANMAT) establishes for the granting of the certificate of free marketing of a medicine. PSMA I&S was used as the active ingredient, whose structure was elucidated by mass spectrometry, in solution with stannous chloride as a reducer. Radiochemical purity was determined by HPLC with C18 column and by ascending radiochromatography, thus evaluating ($^{99m}$Tc)-PSMA, colloid and ($^{99m}$Tc)-free. Preclinical studies evaluated the pharmacokinetic and pharmacodynamic behavior of ($^{99m}$Tc)-PSMA and supported its clinical use. All patients who joined the clinical study (phase I completed and phase II in development) had previous determination of the disease and the images were compared against ($^{68}$Ga)-PSMA, as the *gold standard*, demonstrating the sensitivity, safety and diagnostic specificity.

**Key words:** ($^{99m}$Tc)-PSMA, ($^{68}$Ga)-PSMA, prostate cancer.

## INTRODUCTION

Prostate cancer is currently one of the most common neoplasms worldwide and has become a major health problem over the past four decades. According to the WHO, one in seven men in the world is diagnosed with prostate cancer in their lifetime (1). In Argentina, approximately 12,000 cases are detected each year (2), which represents approximately 9% of total tumors (2). At diagnosis, approximately 50-70% of patients are locally advanced, and approximately 15-30% have bone metastases. Since prostate cancer is androgen-dependent, the initial treatment for advanced/metastatic disease remains suppression of testicular androgen production. Although approximately 80% initially respond to hormonal treatment for 18 to 24 months, most subsequently relapse, and prostate cancer usually progresses from androgen-dependent to an independent state (3). An increase in prostate-specific antigen (PSA) levels, free or conjugated, progressive clinical symptoms, and/or magnetic resonance imaging (MRI) or bone scintigraphy studies with technetium-99m ($^{99m}$Tc) labeled diphosphonates are indicators of androgen deprivation failure (3) and most forms of treatment for hormone-refractory prostate cancer are aimed only at improving the quality of life of patients and not to cure it (4). Today, conventional methods of prostate imaging are computed tomography (CT),

MRI, ($^{18}$F)-choline, and more recently ($^{68}$Ga)-PSMA, the latter two using PET technology. Both technetium-99m ($^{99m}$Tc) and ($^{18}$F)-choline-labeled diphosphonates target non-specific membrane receptors, and it is extremely difficult to correlate the diagnosis with PSA levels, which is an indicator of the level of tumor aggressiveness according to the Gleason classification (5).

PSMA is a type II transmembrane protein present in all prostate tissues but is exacerbated in prostate cancer (6) and its metastases (7, 8). Histochemical studies have shown that PSMA expression increases in cases where the disease is differentiated, metastatic, or hormone-resistant (9) and its expression level is a significant prognosis for disease outcome (10). The PSMA, with a molecular weight of 100 kDa, consists of 750 amino acids and has a structure made up of three regions; namely, an extracellular one of 707 amino acids divided into three zones of which one is rich in proline and glycine, another with no known function and a third where the binding sites of PSMA inhibitory molecules are located. The second region, composed of 24 amino acids, is integrated into the cell membrane and the third is a cytoplasmic tail containing 19 amino acids in which monoclonal antibodies of the 7E11 type have been shown to interact (11). Over the past decade, the development of molecules targeting this specific antigen in the prostate membrane has become a substantial part of prostate cancer imaging and/or therapy, spanning a variety of applications ranging from SPECT and PET diagnostics to theragnostic and therapeutic methods (12, 13) to such an extent that today it tends to be the preferred method for the detection of lesions in biochemical relapse after primary treatment (14, 15, 18, 19, 20, 21). In many countries, including Argentina, access to diagnosis using PET technology can be difficult. Therefore, the potential use of technetium-99m (99mTc)-labeled radiopharmaceuticals in the management of prostate cancer is increasingly needed (22, 23).

The objective of this work is to carry out the comprehensive development of a set of reagents, the ($^{99m}$Tc)-PSMA, following the regulations of the National Administration of Drugs, Food and Medical Technology (ANMAT). To this end, we start with the chemical characterization of the active ingredient, the labeling and quality control, the performance of preclinical studies and phase I and II clinical studies using ($^{68}$*Ga*)-PSMA as the gold standard, in the latter.

## MATERIALS AND METHODS

### 1.- Active ingredient

The active substance is Glu-CO-Lys[(Sub)DLys-D2Nal-DTyr-mas3] trifluoroacetate or PSMA I&S provided by ABX. According to the ANMAT, the chemical structure must be elucidated, which was done by mass spectrometry, which was measured on a solution

of water-acetonitrile-formic acid using a Bruker microOTOF-Q II spectrometer with electrospray ionization in positive mode.

**2.- Elaboration of the set of lyophilized reagents, its labeling with sodium pertechnetate solution ($^{99m}$Tc), quality controls and clinical studies.**

A set of reagents was prepared under GMP conditions containing in lyophilized form: 80 µg PSMA I&S, 25 µg anhydrous stannous chloride, 5 mg sodium tartrate, 30 µg ascorbic acid and 20 mg mannitol. It was reconstituted with 1110 MBq (30 mCi) of sterile, bacterial endotoxin-free radioactive solution of sodium pertechneciate ($^{99m}$Tc) heated to 90-95 °C for 10 minutes and allowed to cool to room temperature. The appearance of the lyophilized and the reconstituted solution, pH, quantification of the active ingredient, radiochemical purity, sterility and absence of bacterial endotoxins were controlled. Radiochemical purity was determined by two ascending radiochromatography systems. The first (A) uses ITLC(SG), as the stationary phase, and methanol:ammonium acetate 1M 1:1 (v:v) as the mobile phase; in this the free ($^{99m}$Tc) and the ($^{99m}$Tc)-PSMA have an Rf between 0.7-1.0 and the colloidal (99mTc) an Rf 0.0; the second (B) uses TLC 60 RP-18 as a stationary phase and acetonitrile:water (1% TFA) 30:70 (v:v) as a mobile phase where the ($^{99m}$Tc)-PSMA and the ($^{99m}$Tc)-colloidal have an Rf between 0.0-0.5 and the ($^{99m}$Tc)-free Rf between 0.7-1.0. HPLC determination used a deactivated octadecylsilyl silica gel column as a stationary phase and a 0.1% TFA A solution in water and a 0.1% TFA B solution in acetonitrile as mobile phases that were used as a gradient in a Shimadzu equipment with UV/visible detector and radiometric detector. Retention times are approximately 8 min for the ($^{99m}$Tc)-PSMA and 2 to 3 min for the free ($^{99m}$Tc). These techniques were also used to assess post-marking stability. The quantification of the active substance in the lyophilized powder was performed by HPLC using a column of octadecylsilyl silica gel deactivated as a stationary phase and a solution A of 0.25 ml TFA in 250 ml of WFI and another B solution of 0.25 ml TFA in 250 ml of HPLC quality acetonitrile; the reference standard solution was 1 mg standard in 1 ml of WFI. The retention time of the reference solution is approximately 8.0 minutes; the retention time of the sample solution should not differ by more than 0.2 min from the reference solution.

**3.- Determination of lipophilic power**

Following the S. Oie technique (24), the results are expressed as the logarithm of the ratio of activity in the organic phase, n-octanol, and non-organic, phosphate buffer 0.1 M. We worked with n=6 and placed 2 ml of n-octanol, 1.9 ml of 0.1M phosphate buffer and 50 µl of ($^{99m}$Tc)-PSMA in a centrifuge tube. It was stirred in a *vortex* for 2 min and centrifuged for 5 min at 5.000 rpm. In 100 µl of each of the phases, the activity was determined, which was expressed as counts per milliliter.

**4.- Stability in human serum**

Following the technique of E. M. Faed (25), ($^{99m}$Tc)-PSMA was incubated with fresh human plasma at 37 °C for 3 hours. We worked (n=6) with 50 µl of ($^{99m}$Tc)-PSMA that were placed in a centrifuge tube with 1,000 µl of human serum and then 500 µl of frozen acetonitrile were added. Then they were stirred in a *vortex* for 15 sec. and centrifuged at 10,000 rpm for 5 min.; the pellet was separated from the supernatant and the activity in each of the fractions was determined, which was expressed as cpm and the percentage of binding in the protein fraction was calculated.

**5.- Cell binding and internalization of the radiopharmaceutical**

Following the technique of Jessie R. (26), human prostate tumor cells (LNCaP) were used. Work (n=6) was done by adding $10^5$ cells in 100 µl of RPMI culture medium, the vials were centrifuged at 3.000 rpm for 5 min at 4°C and the culture media were removed; the cell pellets were washed with 200 µl of PBS buffer pH 7.4, 25 µl of ($^{99m}$Tc)-PSMA were added and incubated for 4 hours at 37 °C; then they were centrifuged and washed three times and the supernatant of the last wash and the cell pellet were measured in a well counter expressing the results as CPM. The results are expressed as a percentage of the total activity bound to the cells. To determine the percentage of internalization, the cell pellet is suspended in a 475 µl buffer, then incubated at 37 °C and centrifuged at 3,000 rpm, determining the activity in the supernatant and the cell pellet.

**6.- Biodistribution in normal biological models and with induced tumors**

We worked with nude BALB/c mice (n=30). The animals were treated in accordance with the regulations in force in Argentina. To produce the tumor models, 6x10 LNCaP cells were resuspended in 200 µL of a 1:1 solution of Matrigel (Corning) and RPMI 1460 culture medium. This was injected into the upper right flank of mice, and tumor growth was monitored for 45 days until a size of 10 mm was obtained. Tumored (n=15) and normal (n=15) animals were administered 100 µl of ($^{99m}$Tc)-PSMA with an average activity of 37 MBq (1 mCi) via the penis or caudal route. They were sacrificed by cervical traction at 30, 60 and 90 minutes after administration, dissecting the organs of interest that were weighed after washing, and the activity determined with a dose calibrator, the results being expressed as a percentage of the administered dose per gram of organ.

**7.- Clinical studies**

A prospective study was carried out that included patients with prostate cancer who had previously prescribed a PET diagnostic study from their treating physician. Patients who sign the informed consent form undergo a PET/CT study with ($^{68}$Ga)-PSMA and a SPECT with ($^{99m}$Tc)-PSMA at an interval of 7 days. It is estimated that the tests will demonstrate a sensitivity and specificity of at least 90% with an acceptable error of 10% for ($^{99m}$Tc)-PSMA compared to ($^{68}$Ga)-PSMA with a significance level of 95% and a loss and rejection rate of 10%. The properties of binary diagnostic tests shall be estimated and

presented with 95% CI, including sensitivity, specificity, positive odds ratio (LR), and negative LR. For all comparisons of sensitivities and specificities, as well as LR, global comparisons will be made initially using the Wald test and then individual comparisons with multiple comparison correlation using the Holm method. Differences in sensitivities and specificities, as well as LRs and their 95% CIs, will be calculated using the Roldán-Nofuentes and Sidaty-Regad methods. The whole-body PET/CT is performed with a General Electric Discovery 710 machine and for the correction of attenuation and for the anatomical localization of the PET findings, it is performed by CT with contrast in a 64-slice tomograph. Patients were studied 60 min after intravenous (IV) administration of 1.48 MBq/kg (0.04 mCi/kg) of ($^{68}$Ga)-PSMA. The SPECT study was performed on a General Electric model NM 630 dual-head machine, LEHR collimator, 1024x256 matrix for images obtained every 30 sec. viewed in 360° matrix 128x128 at 180 min after intravenous (IV) administration of 555-740 MBq (15-20 mCi) of ($^{99m}$Tc)-PSMA.

**RESULTS**

**1.- Elucidation of the molecular structure of the active ingredient:** the quasimolecular ion [M+H]+ at m/z 1299.544 (calculated for C59H83N10O21S+ 1299.5499, deviation 0.3 ppm) is observed. The relative abundance of the ions M+H to M+H+4 is consistent with the isotopic distribution by the natural abundance of the isotopes of the elements present in the formula. The pseudopeptide sequence analysis was performed from the EM/EM spectrum on the $[M+H]^+$ ion. The highest mass fragments correspond to sequential water losses at m/z 1281.5328 (M+H-H2O, C59H81N10O20S+, calculated 1281.5344 and at m/z 1263.5167 (M+H-2H2O, C59H79N10O19S+, calculated 1263.5238 probably from serines. The other identified fragments and the breakdown scheme of the molecule are shown below (calculated formulas and masses are indicated in parentheses) (Figure 1).

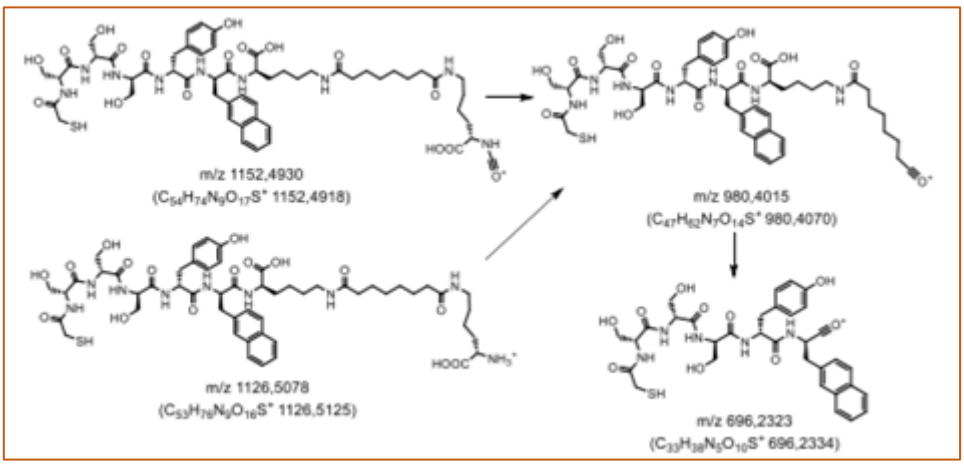

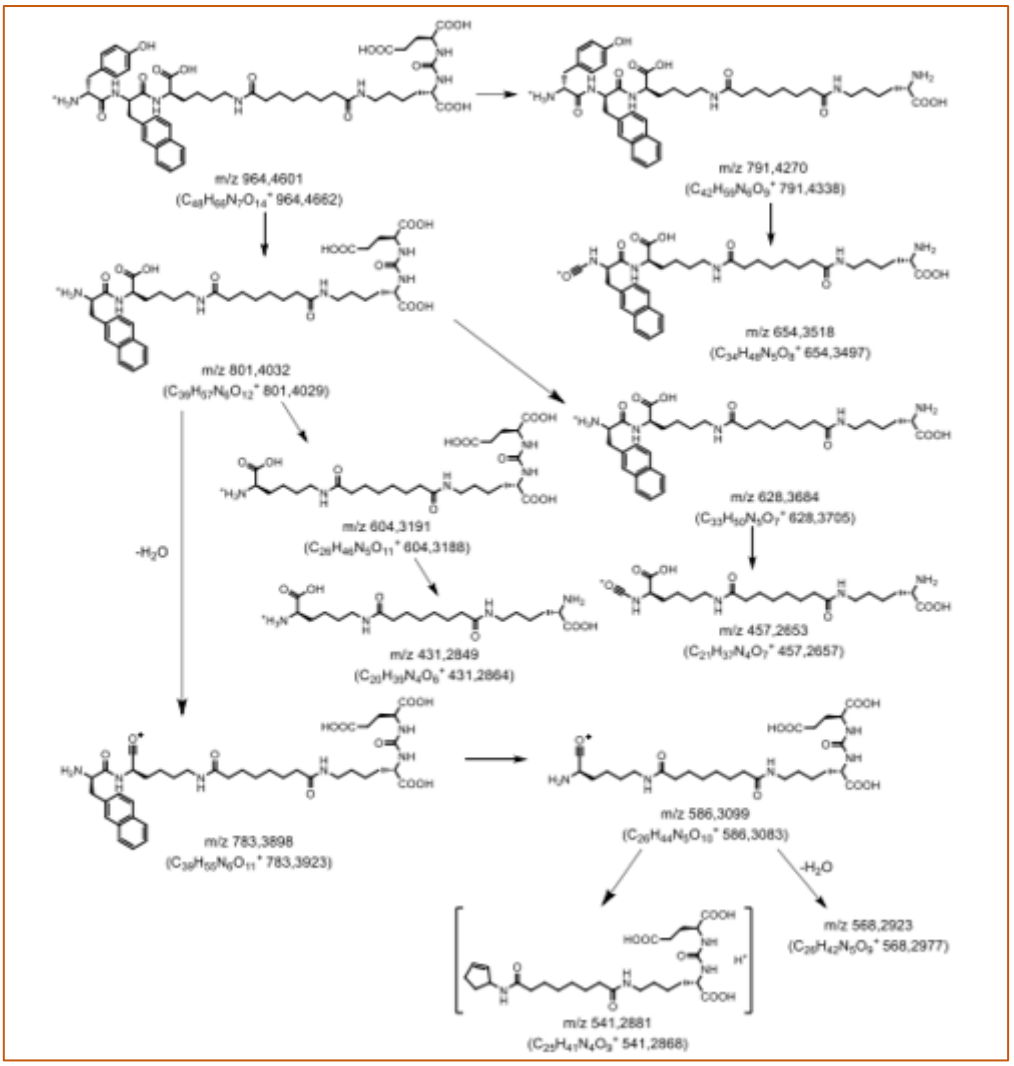


Figure 1

From the sequence of fragments, the formulas of each of the residues of the pseudopeptide can be identified in the order consistent with the structure. Fragments from the C-terminal end show losses of glutamic acid and N-carbonylglutamic acid, and from those fragments the sequential losses of lysine and suberyl-lysine. From the N-terminal end, the initial loss of the *N-thioacetyl-triserine* fragment is observed, followed sequentially by the losses of tyrosine and ß-naphthyalanine. In addition, several fragments with combined residue losses from both ends are observed that are only compatible with the sequence *N*-(*2-mercaptoacetyl*)D-Ser-D-Ser-D-D-Tyr-D-ß-(2-naphthyl)Ala-D-Lys-(SUB-L-Lys-Urea-L-Glu). In conclusion, the spectroscopic data are consistent with the structure proposed by the provider.

**2.- Elaboration of the set of lyophilized reagents, its labeling with sodium pertechneciate solution ($^{99m}$Tc) and quality controls:** The qualitative-quantitative formulation used allowed us to obtain, under GMP conditions, a lyophilized powder that has a radiochemical purity of more than 95%. In the labeling reaction, technetium-99m

($^{99m}$Tc) acts in an oxidation state V ($^{99m}$Tc=O3+) where the d2 configuration has two electrons th*at coordinate with the electron-giving region of the PSMA I&S, giving high stability to the radiopharmaceutical molecule (Figure 2, blue circle)*

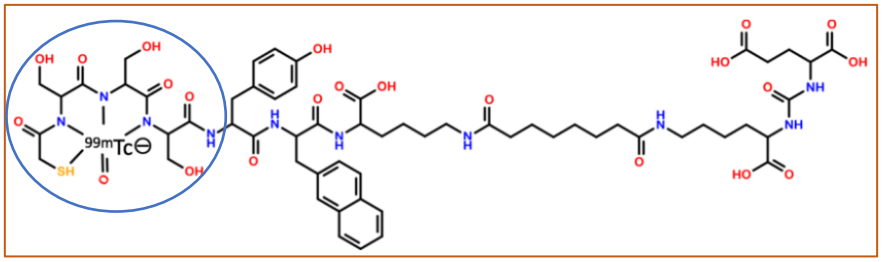

Figure 2

The determination of radiochemical purity by thin layer radiochromatography was efficient in determining the percentages of ($^{99m}$Tc)-PSMA, ($^{99m}$Tc)-free and colloidal states; these results agreed with those obtained by HPLC. These systems allowed us to determine that the stability of the labeled compound was 6 hours post-labeling and that the stability of the lyophilized kit was, to date, 180 days post-processing, during which period not only radiochemical purity was maintained, but also sterility and apirogenicity. Regarding the quantification of the active ingredient in the lyophilized powder, it was consistent with what was proposed in the qualitative-quantitative formulation.

**3.- In vitro studies:** the lipophilicity of ($^{99m}$Tc)-PSMA, expressed as a logarithm of the partition coefficient between n-octanol and phosphate buffer, was -4.62±0.01, which indicates that it is a water-soluble molecule and, therefore, hydrophilic in nature. The stability of ($^{99m}$Tc)-PSMA in fresh human serum showed that after three hours it was 51.8±0.03%. PSMA receptor binding in cell cultures carrying prostate tumors was 53.6±0.66%, while the percentage of internalization was 43.09±0.02%, which means that 84% of the radiopharmaceutical bound to cell receptors is internalized.

**4.- In vivo studies:** biodistribution studies in normal biological models at 30, 60 and 90 minutes after administration showed a preponderant renal excretion of the radiopharmaceutical (Figure 3). Data are expressed as a percentage of the dose administered per gram of organ.

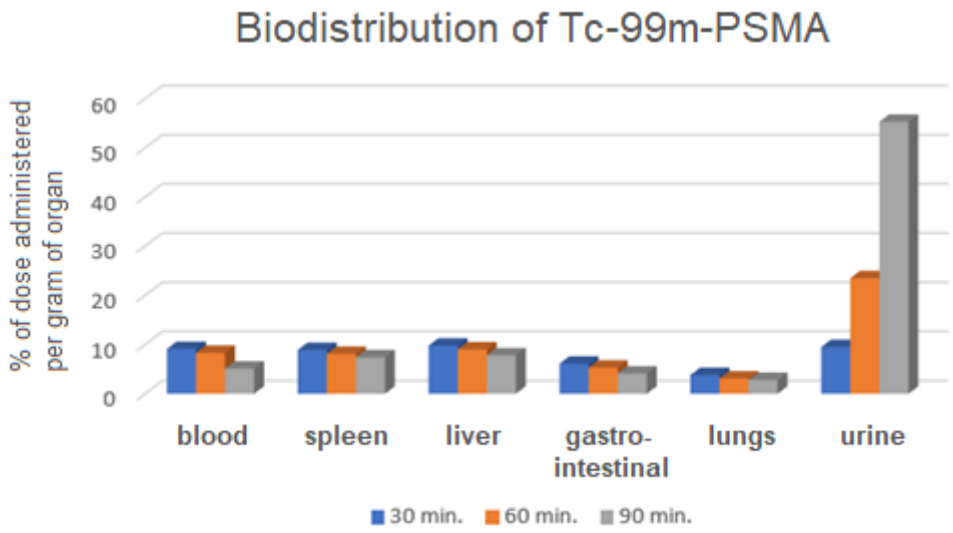


Figure 3

Tumor uptake of ($^{99m}$Tc)-PSMA was assessed only 90 minutes after administration of the ($^{99m}$Tc)-PSMA dose and was 7.81±2.17% of the dose administered per gram of tumor, while the tumor vs. muscle ratio was 23.44%.

**5.- Clinical studies:** so far, 18 patients aged between 56 and 75 years old (average 68.8 years old) have been evaluated. Figure 4A shows that 58.4% of the patients evaluated had been prostectomized and 41.60% had received radiotherapeutic treatments; Figure 4B shows that 58.40% had a high to very high Gleason index (greater than 8) while 41.60% had a low to intermediate Gleason index; Figure 4C shows that 44.5% of the patients had skeletal and extraskeletal disease, while 22.20% had exclusively skeletal disease and 33.30% had lymph node disease; None of the patients in the current population had visceral metastases.

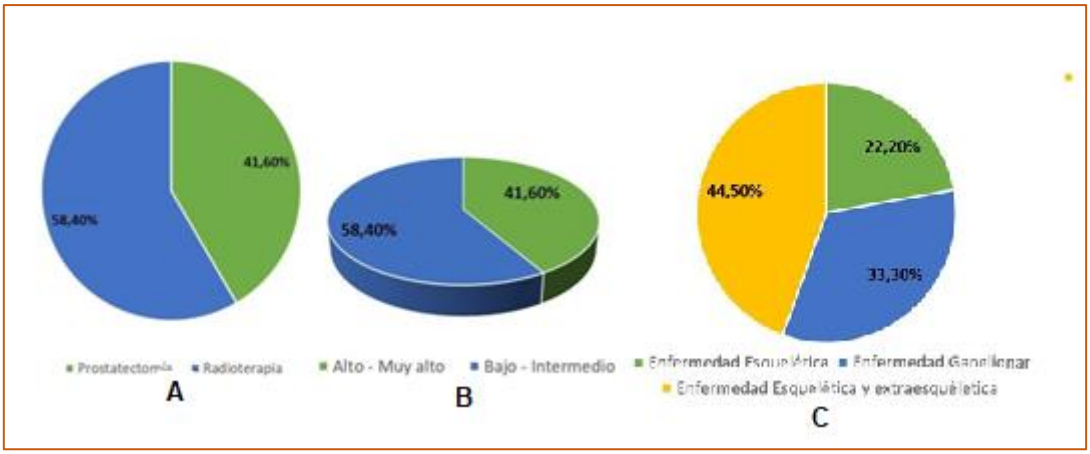


Figure 4

Figure 5 shows the comparative biodistribution of both radiopharmaceuticals in a 60-year-old patient with prostate cancer and Gleason index 8. Overexpression of both radiopharmaceuticals is observed in a lymph node structure of the left internal iliac chain

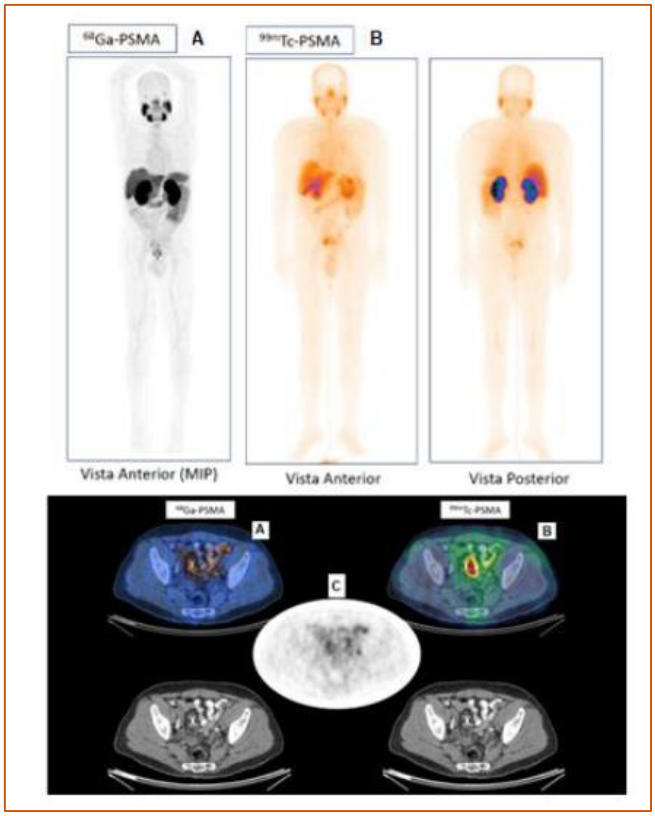


Figure 5: A: $^{68}$Ga-PSMA; B:$^{99m}$Tc-PSMA; C: Image Fusion

Figures 6 and 7 show a 67-year-old patient with prostectomized prostate cancer and a high Gleason index. Figure 6A shows the axial and appendicular image with ($^{99m}$Tc)-PSMA, while image B shows the uptake with ($^{68}$Ga)-PSMA. A high correlation of skeletal metastatic lesions is observed. Figure 7 shows the sagittal slices of the same patient; in 7A, uptake of ($^{99m}$Tc)-PSMA, in 7B, morphological lesions by CT, and in 7C, uptake of ($^{68}$Ga)-PSMA, evidencing metastatic involvement in vertebral bodies.

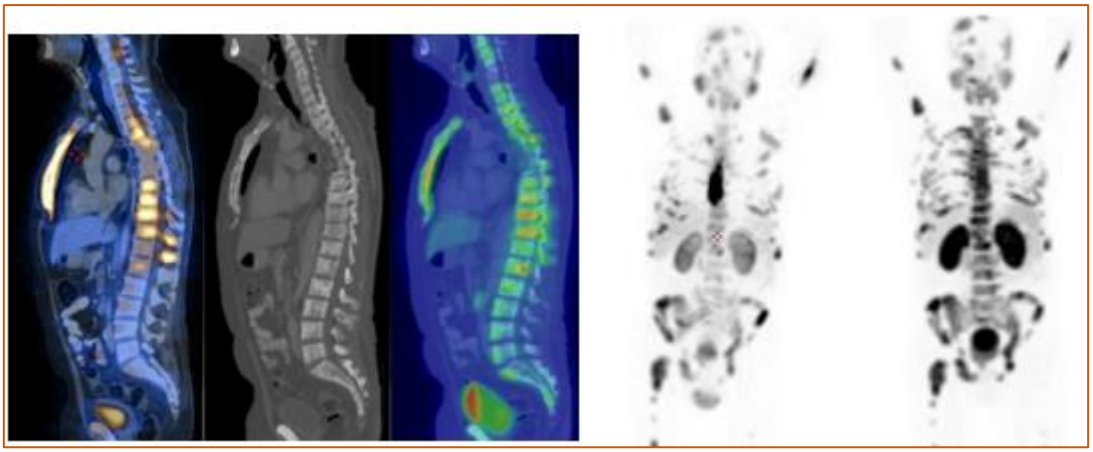

Figure 6 Figure 7

## DISCUSION

As previously indicated, the main objective of this work was to develop a kit of reagents for labelling with technetium-99m ($^{99m}$Tc) that allows the evaluation of primary and/or metastatic prostatic tumors. This development, as it has been carried out by a radiopharmaceutical company, had to be carried out in accordance with the regulations in force at ANMAT. The formulation used, as well as the quality control methods and "in *vitro"* and *"in vivo" studies* allowed us to administer it to patients safely. Bone metastases are one of the most common manifestations in patients with prostate cancer and bone scintigraphy with ($^{99m}$Tc)-HDP or ($^{99m}$Tc)-MDP is usually used to detect it; however, false-positive results are common due to uptake in a variety of benign bone lesions and, consequently, overall specificity is low (27). In one study (n=25), SPECT/CT imaging with ($^{99m}$Tc)-PSMA found 95 bone metastases, which was superior to other imaging modalities such as bone scintigraphy and magnetic resonance imaging (28). The work of B. Albalooshi *et al*. (29) demonstrated that ($^{99m}$Tc)-PSMA scanning is as sensitive as ($^{68}$Ga)-PSMA scanning in prostate cancer patients in terms of detecting abnormalities, lymph node metastases, or skeletal involvement; however, it is less sensitive in detecting lesions in the prostate bed. In our case, all lesions visualized with ($^{99m}$Tc)-PSMA have similar representation in those obtained with ($^{68}$Ga)-PSMA, and in the case of discordant lesions with less scintigraphic representation, they are linked to size/resolution, as well as to the density of prostate-specific antigen in tumor prostate cells. However, the joint SNM/NMD guideline on PET/CT with ($^{68}$Ga)-PSMA recommends it for the localization of recurrence in patients with PSA levels of 0.1 to 10 ng/mL (30). Our work is in the process of demonstrating the correlation of the data described, SUVs and other variables.

## CONCLUSIONS

Considering the limited availability and high cost of ($^{68}$Ga)-PSMA PET/CT, SPECT/CT imaging of prostate cancer with ($^{99m}$Tc)-PSMA should be considered as a good alternative. Analyzing the costs and facilities of performing PET/CT with (68Ga)-PSMA and SPECT/CT with ($^{99m}$Tc)-PSMA shows that the use of ($^{99m}$Tc)-PSMA SPECT/CT in the treatment of prostate cancer patients will have a significant impact on the health economics of prostate cancer. Finally, the central objective of this work was fulfilled since the monographic dossier that will lead to the obtaining of the certificate of free sale was presented for consideration by ANMAT while the clinical evaluation continues through the analysis of the results obtained from the multicenter studies that will be carried out to complete phases III, IV and V.

Bibliography

1.- Litwin MS, et al. The Diagnosis and Treatment of Prostate Cancer: A Review. Jama. 2017 Jun 27; 317(24):2532-42.

2.- International Agency for Research on Cancer (IARC) and Global Cancer Observatory (GLOBOCAN).

3.- Kazutoshi Frujita et al. Role of androgen receptor in prostate cancer: A review. World J. Mens Health. 2019; Sep 37(3).288-295.

4.- Seth A. et al. Effect of Chemotherapy With Docetaxel With Androgen Suppression and Radiotherapy for Localized High-Risk Prostate Cancer: The Randomized Phase III NRG Oncology RTOG 0521 Trial. J.Cli. Oncology. 2019; May. 1159-1168

5.- Batool Albalooshi, et al Direct comparison of 99mTc-PSMA SPECT/CT and 68Ga-PSMA PET/CT in patients with prostate cancer. A.O.J.Nucl.Med.Biol.; 2020. Dec 8 (1).

6.- Silver DA, Pellicer I, Fair WR, Heston WD, Cordon-Cardo C. Prostate-specific membrane antigen expression in normal and malignant human tissues. Clin Cancer Res. 1997; 3:81–5.

7.- Bostwick DG, et al. Prostate specific membrane antigen expression in prostatic intraepithelial neoplasia and adenocarcinoma: a study of 184 cases. Cancer. 1998; 82:2256–61.

8.- Mannweiler S, et al. Heterogeneity of prostate-specific membrane antigen (PSMA) expression in prostate carcinoma with distant metastasis. Pathol Oncol Res. 2009; 15:167–72

9.- Tobias Maurer et al. Current use of PSMA-PET in prostate cáncer management. Nature Reviews Urology 13 (4). February 2016.

10.- Fendler WP, et al. 68Ga-PSMA PET/CT: Joint EANM and SNMMI procedure guideline for prostate cancer imaging: version 1.0. Eur J Nucl Med Mol Imaging. 2017; 44:1014–24.

11.- Hellwig D, et al. Survey on the range of indications for PET diagnostics in Germany. Nuclear medicine. 2019; 58:V75.

12.- Lütje S, et al. PSMA ligands for radionuclide imaging and therapy of prostate cancer: clinical status. Theranostics. 2015; 5:1388–1401.

13.- Maurer T, et al. Current use of PSMA-PET in prostate cancer management. Nat Rev Urol. 2016; 13:226–235.

14.- Maresca KP, et al. Small molecule inhibitors of PSMA incorporating technetium-99m for imaging prostate cancer: effects of chelate design on pharmacokinetics. Inorg Chim Acta. 2012; 389:168–175.

15. Vallabhajosula S, et al. 99mTc-labeled small-molecule inhibitors of prostate-specific membrane antigen: pharmacokinetics and biodistribution studies in healthy subjects and patients with metastatic prostate cancer. J Nucl. Med.2014; 55:1791–1798.
16.- Eder M, et al. Ga-68-complex lipophilicity and the targeting property of a urea-based PSMA inhibitor for PET imaging. Bioconjug Chem, 2012; 23:688–697.
17.- Afshar-Oromieh A, et al. The diagnostic value of PET/CT imaging with the 68Ga-labelled PSMA ligand HBED-CC in the diagnosis of recurrent prostate cancer. Eur J Nucl Med Mol Imaging. 2015; 42:197–209.
18.- Mease RC, et al. N-[N-[(S)-1,3-dicarboxypropyl]carbamoyl]-4-[F-18]fluorobenzyl-L-cysteine, [F-18]DCFBC: a new imaging probe for prostate cancer. Clin Cancer Res. 2008; 14:3036–3043.
19.- Rowe SP, et al. 18F-DCFBC PET/CT for PSMA-based detection and characterization of primary prostate cancer. J Nucl Med. 2015; 56:1003–1010.
20.- Chen Y, et al. 2-(3-{1-Carboxy-5-[(6-[18F]fluoro-pyridine-3-carbonyl)-amino]-pentyl}-ureido)-pentanedioic acid, [18F]DCFPyL, a PSMA-based PET imaging agent for prostate cancer. Clin Cancer Res. 2011; 17:7645–7653.
21.- Szabo Z, et al. Initial evaluation of [18F]DCFPyL for prostatespecific membrane antigen (PSMA)-targeted PET imaging of prostate cancer. Mol Imaging Biol. 2015; 17:565–574.
22.- Su H-C, et al. Evaluation of 99mTclabeled PSMA-SPECT/CT imaging in prostate cancer patients who have undergone biochemical relapse. Asian J Androl. 2017; 19:267
23.- Robu S, et al. Preclinical evaluation and first patient application of 99m Tc-PSMA-I&S for SPECT imaging and radioguided surgery in prostate cancer. J Nucl Med. 2017; 58:235–42.
24.- S. Oie. Drug distribution and binding. J Clin Pharmacol;1986. Nov-Dec; 26(8):583-586.
25.- E.M.Faed. Protein binding of drugs in plasma, interstitial fluid and tissues: Effect on pharmacokinetics. E.J.Cli.Pharmacology. 1981; 21:77-81
26.- Jessie R. et al. PSMA-targeted SPECT agents: Mode of Binding effect on in vitro Performance. Prostate. 2013 Mar; 73(4): 355–362.
27.- Langsteger W, et al. Beheshti M. (18)F-NaF-PET/CT and (99m)Tc-MDP Bone Scintigraphy in the Detection of Bone Metastases in Prostate Cancer. Sem.Nucl. Med. 2016 Nov; 46(6):491-501.
28.- Su HC, Zhu, et al. Evaluation of 99mTc-labeled PSMA-SPECT/CT imaging in prostate cancer patients who have undergone biochemical relapse. Asian J. Andrology. 2017 May-Jun; 19(3):267-71.
29.- B. Albalooshi et al. Direct comparison of 99mTc-PSMA SPECT/CT and 68Ga-PSMA

PET/CT in patients with prostate cancer. Asia Ocean J.Nucl.Med.Biol. 2020; 8:1-7.
30.- Fendler WP, et al. 68Ga-PSMA PET/CT: Joint EANM and SNMMI procedure guideline for prostate cancer imaging: versión 1.0. European journal of nuclear medicine and molecular imaging. 2017 Jun; 44(6):1014-24.